

# Contribution of GRB Emission to the GeV Extragalactic Diffuse Gamma-Ray Flux

S. Casanova and B. L. Dingus

*Los Alamos National Laboratory, Los Alamos, NM 87545*

and

Bing Zhang

*Physics Department, University of Nevada Las Vegas, NV 89154*

## ABSTRACT

TeV gamma rays emitted by GRBs are converted into electron-positron pairs via interactions with the extragalactic infrared radiation fields. In turn the pairs produced, whose trajectories are randomized by magnetic fields, will inverse Compton scatter off the cosmic microwave background photons. The beamed TeV gamma ray flux from GRBs is thus transformed into a GeV isotropic gamma ray flux, which contributes to the total extragalactic gamma-ray background emission. Assuming a model for the extragalactic radiation fields, for the GRB redshift distribution and for the GRB luminosity function, we evaluate the contribution of the GRB prompt and scattered emissions to the measured extragalactic gamma-ray flux. To estimate this contribution we optimistically require that the energy flux at TeV energies is about 10 times stronger than the energy flux at MeV energies. The resulting gamma-ray diffuse background is only a small fraction of what is observed, allowing blazars and other sources to give the dominant contribution.

*Subject headings:* 98.70.Rz

## 1. Introduction

The nature of the extragalactic gamma ray background emission has been a topic of great interest since EGRET collaboration evaluated its spectrum in the range from 30 MeV to 100 GeV (Sreekumar et al. 1998). The diffuse emission coming from beyond the galaxy was determined by subtracting the contributions of resolved point sources, the diffuse galactic

emission, and the instrumental background from the gamma-ray intensities observed by EGRET. The emission is found to be a power law in energy

$$\frac{dN_\gamma}{dA dt d\Omega dE} = (7.32 \pm 0.34) \times 10^{-6} \left( \frac{E}{0.451 \text{ GeV}} \right)^{-2.10 \pm 0.03} \text{ cm}^{-2} \text{ s}^{-1} \text{ sr}^{-1} \text{ GeV}^{-1} \quad (1)$$

and is highly isotropic on the sky. Mukherjee & Chiang (1999) suggested that blazars can explain up to 25 per cent of the extragalactic emission. The hypothesis that the flux is predominantly due to blazars seems to be reinforced by a new evaluation of the extragalactic emission (Strong et al. 2004) which is slightly lower and steeper than that found by Sreekumar et al. (1998). The result is not consistent with a power law and shows some positive curvature which the authors relate to an origin in blazars emission. Kneiske & Mannheim (2005) recently suggested that up to 85 per cent of the extragalactic emission could arise from blazars. According to Stecker & Salamon (1996, 2001) blazars can account for the entire extragalactic  $\gamma$ -ray background observed by EGRET. Above 100 MeV normal galaxies contribute from 3 to 10 per cent of the observed diffuse extragalactic flux. However from the analysis of (Erlykin & Wolfendale 1995) the spectrum of normal galaxies seems to differ from the extragalactic diffuse emission spectrum. Dar & Shaviv (1995) have suggested that the extragalactic diffuse arises from cosmic rays interacting with intergalactic gas. This contribution seems to disagree with the diffuse gamma ray spectrum according to Stecker & Salamon (1996). Loeb & Waxman (2000) suggested fossil radiation from shock accelerated cosmic rays during structure formation as possible contribution. Stawarz et al. (2006) have estimated that inverse Compton scattering of starlight photon fields by the ultrarelativistic electrons in kiloparsec-scale jets in FR I radio galaxies contributes about one percent to the EGRET extragalactic flux. Chi & Wolfendale (1989) and Wdowczyk & Wolfendale (1990) have shown that upscattering of CMB to  $\gamma$ -ray energies by cosmic ray electrons and protons does not provide a significant contribution to the diffuse extragalactic emission.

However, the question about the origin of the extragalactic emission is still open and can possibly be solved by admitting that different sources contribute to it. In fact all unresolved discrete sources outside the Galaxy contribute to the extragalactic background emission; the problem is clearly to understand how big the different contributions are. As already pointed out by Hartmann et al. (2003), who considered GRBs as a source for the diffuse gamma-ray emission at MeV energies, prompt and delayed emissions from GRBs should also contribute to the diffuse extragalactic emission, especially if some GRBs emit photons in the GeV-TeV energy. In fact, outside the GRB source, due to interactions with cosmic infra-red background photons, most of the high energy GRB photons produce high-energy electron-positron pairs. The pairs inverse Compton scatter off CMB photons and produce secondary photons, which in turn interact with IR photons and generate other pairs. Multiple inverse Compton scatterings occur until the energy of the secondary photons is no longer large

enough to trigger pair production with the IR photons. When the energy of the scattered photons is not sufficient to produce a subsequent pair, the photons travel to the Earth without undergoing further absorption. After multiple pair-production and inverse Compton processes, the initial energy of the TeV photons escaping the GRBs will have been shifted to MeV-GeV energies (Coppi & Aharonian 1997; Plaga 1995; Dai & Lu 2002; Wang et al. 2004; Razzaque et al. 2004). The data on extragalactic diffuse emission in the MeV-GeV energy range are thus useful to put constraints on high energy emission from gamma ray bursts at GeV-TeV energy.

In the following we assume a flat cosmological model with normalized Hubble constant  $h = 0.71$ , with  $\Omega_m = 0.3$  and  $\Omega_\Lambda = 0.7$ . Cosmological distances and volumes are calculated following Hogg (1999).

## 2. GRB model

Gamma ray bursts are cosmological spots of short, intense and narrowly beamed  $\gamma$ -ray emission, whose observed isotropic luminosities,  $L_{iso}$ , are in the range of  $10^{51} - 10^{52}$  erg/s. The huge energy released by GRBs is almost certainly produced by ultra-relativistic flows, whose bulk Lorentz factors  $\Gamma_b$  may vary in the range of 100 and 1000, with a typical value of 300 (Baring & Harding 1997; Lithwick & Sari 2001; Zhang et al. 2006). The widely accepted fireball internal-external shock model for GRBs envisages that high energy protons and electrons are accelerated in shocks by interaction with magnetic fields. The process of Fermi acceleration leads to electron and proton power-law spectra of index between -2 and -3. Electrons and protons cool through synchrotron emission. Since the electron cooling time is shorter than the proton cooling time, as a first approximation, the GRB prompt spectrum is believed to be dominated by electron synchrotron emission only. The observed prompt spectrum arising from electron synchrotron emission is a Band function (Band et al. 1993), proportional to  $E^\alpha$  below the synchrotron peak energy,  $E_{pk}$ , with  $\alpha$  about -1 and to  $E^\beta$  above the peak energy, with  $\beta$  usually between -2 and -3. Below the synchrotron self absorption energy,  $E_{ssa}$ , low energy photons are absorbed by fireball electrons in a magnetic field by synchrotron self-absorption.

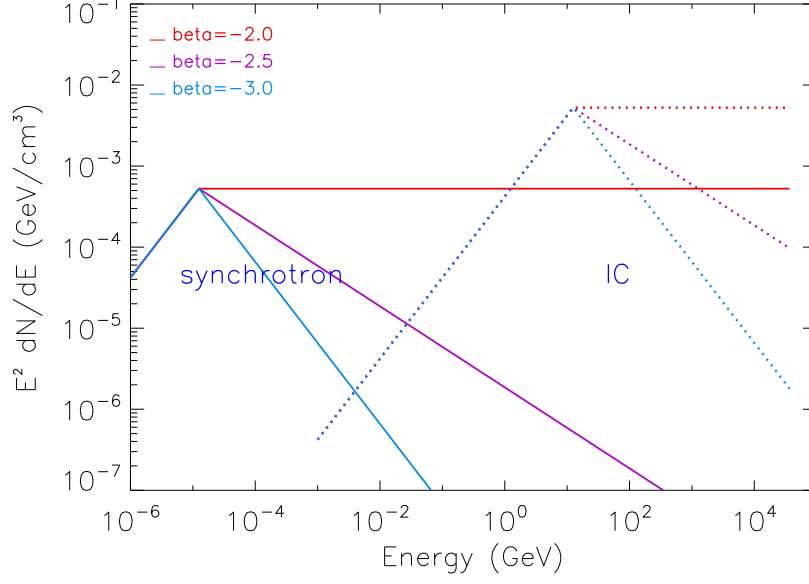


Fig. 1.— Band spectrum and Inverse Compton spectrum for a GRB having isotropic luminosity  $10^{52}$  erg/s and located at  $z = 0.1$ . The slope  $\alpha = -1$  and  $\beta$  varies between -2 and -3 for both synchrotron and IC spectra. The ratio  $r$  between the synchrotron peak flux and the TeV emission peak flux is assumed to be 10.

High energy (up to TeV) emission has been detected in some GRBs (Gonzales et al. 2003; Hurley et al. 1994; Atkins et al. 2003). According to the fireball model, TeV photons can be produced in both internal (Dai & Lu 2002; Razzaque et al. 2004) and external (Zhang & Mészáros 2001; Böttcher & Dermer 1998) shocks, either through electron inverse Compton or proton synchrotron emission. Wang et al. (2001) proposed that the cross inverse Compton scattering between the photons and electrons in forward and reverse shocks can also produce TeV photons. TeV photons can be also generated through inverse Compton scattering of shock accelerated particles in external shocks off a bath of photon that overlaps the shocked region. The photon bath could be either the prompt gamma-ray emission itself (Beloborodov 2005; Fan et al. 2005) or the late-time X-ray flares (Wang & Mészáros 2006). For such distant sources as GRBs, TeV photons are mostly absorbed through pair production with cosmic background radiation (CBR), but some indications of TeV gamma rays from GRBs at low redshift were provided by experiments like Milagro (Atkins et al. 2000), HEGRA (Padilla et al. 1998) and Tibet (Amenomori et al. 1996). In our calculation TeV prompt energy photons are taken into account in the prompt spectrum without investigating the details of the way they are created. We model the GRB prompt TeV emission as an additional broken power law with low energy spectral index  $\alpha = -1$  and high energy spectral index  $\beta = -2$ . The synchrotron peak energy  $E_{pk}$  depends on the isotropic energy of the burst (Amati et al. 2002). In order to match the typical observed  $E_{pk}$  at 100 keV - 1 MeV, the typical random electron Lorentz factor  $\gamma_e$  is about 300-1000. Since most high energy emission components are related to inverse Compton (IC) scattering, we design our high energy component to mimic the IC in the internal shocks. The typical separation between the synchrotron typical frequency and the IC typical frequency is  $\gamma_e^2$ , which varies between  $10^5$  and  $10^6$ . So the break energy of the additional TeV component is chosen to be around  $10^5$  times the synchrotron peak  $E_{pk}$  (Zhang & Mészáros 2002a). The relative energies contained in the synchrotron component and the IC component depend on the IC  $Y$ -parameter (Panaiteescu & Kumar 2000; Sari & Esin 2001; Zhang & Mészáros 2001)

$$Y = \frac{L_{IC}}{L_{syn}} \sim \sqrt{(\epsilon_e/\epsilon_B)} \quad (2)$$

for  $\epsilon_e \gg \epsilon_B$ , where  $\epsilon_e$  and  $\epsilon_B$  are shock energy equipartition parameters for electrons and magnetic fields, respectively. Because of a possible Klein-Nishina limitation, this  $Y$  parameter could not be too high. An optimistic value would be around 10, corresponding to  $\epsilon_e \sim 100\epsilon_B$  (see Fig. 1). This requires that the GRB internal shocks are not very magnetized<sup>1</sup>.

---

<sup>1</sup>Some evidence however suggests a magnetized central engine (Zhang et al. 2003; Fan et al. 2002; Kumar & Panaiteescu 2003). In that case, the IC component is at most comparable to the synchrotron component.

GRB emission is likely narrowly beamed. The jet may be top-hat shaped with uniform energy distribution inside the jet cone and a sharp drop off at the edge (Rhoads 1999; Sari et al. 1999) or “structured” with angle-dependent energy density inside the jet (Zhang & Mészáros 2002b; Rossi et al. 2002). The total amount of emission energy corrected for the beaming effect is likely standard, about  $1.3 \times 10^{51}$  erg (Frail et al. 2001). The average beaming factor ranges in the literature from around 75 (Guetta et al. 2005) to 500 (Frail et al. 2001).

Photon-photon absorption through pair production inside the GRB source region controls the range in energy and the amount of radiation emitted. Our following treatments closely follow Razzaque et al. (2004). In Fig. 2 we plot the optical depths corresponding to the different processes taking place inside the GRB source region,  $\gamma\gamma$  absorption, electron Compton scattering and  $e\gamma \rightarrow e^\pm$ . The GRB isotropic luminosity is  $L_{iso} = 10^{52}$  erg/s and the observed time variability is  $\delta t = 0.01$  s. The time variability is an important parameter for the description of gamma ray bursts. In fact the shock radius

$$r_{sh} = 2 c \delta t \Gamma_b^2 \quad (3)$$

is proportional to the time variability  $\delta t$  and the peak volume number density of photons is defined as

$$n'_\gamma = \frac{L_{iso}}{4 \pi r_{sh}^2 c \Gamma_b E_{pk}}. \quad (4)$$

As shown in Fig. 2,  $\gamma\gamma$  pair production within the GRB attenuates the prompt spectrum, while electron Compton scattering and  $e\gamma \rightarrow e^\pm$  have optical depths less than 1 for the typical parameter sets we are adopting. The optical depth for  $\gamma$ -ray absorption through pair production is the integral above the synchrotron self absorption energy  $E'_{ssa}$  and below the Klein Nishima limit energy  $E'_{KN} = \Gamma_b m_e \gamma'_{emax}$  where the maximum electron Lorentz factor is  $\gamma'_{eKN} = \frac{3e}{\sigma_T B(1+Y)}$ . (Dai & Lu 2002)

$$\tau_{grb} = \frac{r_{sh}}{\Gamma_b} \int_{E'_{ssa}}^{E'_{max2}} \sigma_{pair} \frac{dN'_\gamma}{dE'_\gamma} dE'_\gamma. \quad (5)$$

In Eq. 5 the cross section for  $\gamma$ - $\gamma$  pair production  $\sigma_{pair}$  is

$$\sigma_{pair} = \frac{3}{16} \sigma_{th} (1 - \beta^2) (2\beta(\beta^2 - 2) + (3 - \beta^4 \log((1 + \beta)/(1 - \beta)))) \quad (6)$$

with

$$\beta = \sqrt{1 - \frac{(m c^2)^2}{E_\gamma \epsilon_{cmb}}}. \quad (7)$$

$\frac{dN'_\gamma}{dE'_\gamma}$  in Eq. (5) is the number density of photons per energy in the comoving frame arising from synchrotron and higher energy processes. The total number density of photons is given as a superposition of different synchrotron and possibly higher energy power law spectra

$$\frac{dN'_\gamma}{dE'_\gamma} = \frac{dN_{1\gamma}'}{dE'_\gamma} + \frac{dN_{2\gamma}'}{dE'_\gamma} + \frac{dN_{3\gamma}'}{dE'_\gamma} + \frac{dN_{4\gamma}'}{dE'_\gamma} \quad (8)$$

where

$$\begin{aligned} \frac{dN_{1\gamma}'}{dE'_\gamma} &= \frac{n'_\gamma}{E'_{pk}} \left( \frac{E'_\gamma}{E'_{pk}} \right)^\alpha && \text{for } E'_{ssa} < E'_\gamma < E'_{pk} \\ \frac{dN_{2\gamma}'}{dE'_\gamma} &= \frac{n'_\gamma}{E'_{pk}} \left( \frac{E'_\gamma}{E'_{pk}} \right)^\beta && \text{for } E'_{\gamma pk} < E'_\gamma < E'_{max} \\ \frac{dN_{3\gamma}'}{dE'_\gamma} &= C \frac{n'_\gamma}{E'_{pk2}} \left( \frac{E'_\gamma}{E'_{pk2}} \right)^\alpha && \text{for } E'_{min} < E'_\gamma < E'_{pk2} \\ \frac{dN_{4\gamma}'}{dE'_\gamma} &= C \frac{n'_\gamma}{E'_{pk2}} \left( \frac{E'_\gamma}{E'_{pk2}} \right)^\beta && \text{for } E'_\gamma > E'_{pk2}. \end{aligned} \quad (9)$$

$E'_{pk}$  and  $E'_{pk2}$  are the synchrotron peak energy and the higher emission peak energy, respectively.  $E'_{ssa}$  is the synchrotron self absorption energy,  $E'_{max}$  is the synchrotron cut off corresponding to the maximum energy the electrons are accelerated to by the Fermi mechanism and  $E'_{KN}$  the IC Klein-Nishima limit.  $E'_{min}$  is the IC-boost of the synchrotron self-absorption frequency. The ratio  $R$  of the high energy component energy flux,  $(E'_{pk2})^2 \frac{dN'_\gamma}{dE'_\gamma}$ , and the synchrotron energy flux,  $(E'_{pk})^2 \frac{dN'_\gamma}{dE'_\gamma}$  at the peaks is given by

$$R = C \frac{E_{pk2}}{E_{pk}}, \quad (10)$$

which is adopted as the most optimistic value  $R \sim 10$  in our calculations (see above for more discussion). Here  $\alpha$  and  $\beta$  are free parameters, which we assume to be  $\alpha = -1$  and  $\beta = -2$ .

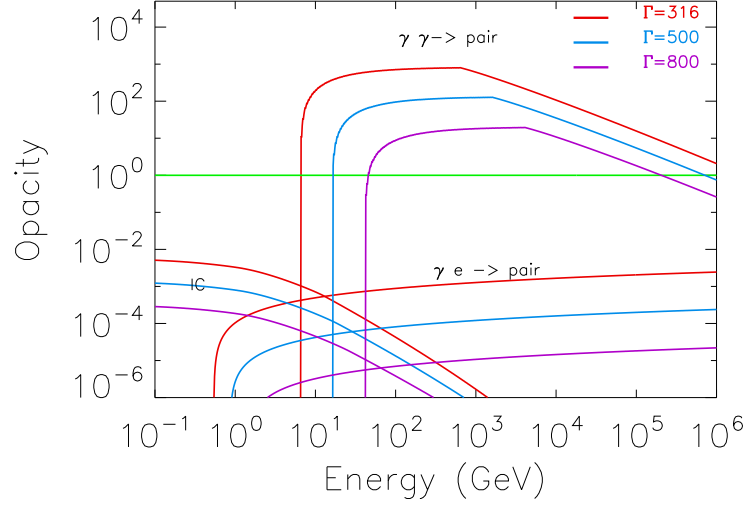


Fig. 2.— Optical depths for processes involving  $\gamma$ -rays in the GRB fireball. Inverse Compton and  $\gamma - e$  pair production do not attenuate the photon spectrum inside the GRB source. The only process attenuating the photon spectrum is  $\gamma$ - $\gamma$  pair production. The attenuation is less efficient for higher bulk Lorentz factors and for shorter variability times. The case of a GRB having isotropic luminosity  $10^{52}$  erg/s and time variability 0.01 second for different bulk Lorentz factors is plotted.



Prompt photons are absorbed above the cutoff energy  $E_{cutoff}$

$$E_{cutoff} = \frac{m_e^2 c^4 \Gamma_b^2}{2 E_{pk}}, \quad (11)$$

corresponding to the photon threshold energy for pair production with lower energy photons. The prompt photons are not absorbed above the so called thinning energy, the photon energy corresponding to optical depth  $\tau_{\gamma\gamma} = 1$

$$E_{thinning} = \frac{3\Lambda L_{iso}\sigma_{TH}m_e^2}{64\pi\Gamma^2\delta t E_{\gamma ssa}^2} \quad (12)$$

where  $\Lambda = \log[2(2E_{\gamma ssa}E_\gamma)^{1/2}]/(m_e\Gamma_b)$ . For high enough bulk Lorentz factors and for short enough time variabilities, GRBs are optically thin at all energies. TeV energy photons emitted by some processes within the GRB will thus be able to leave the source and be observed by experiments like Milagro.

### 3. Photon absorption off IR photon fields

High energy gamma rays are attenuated also when travelling to us because they form pairs in collisions with low energy photons from the meta-galactic radiation field. Following Kneiske et al. (2004), the optical depth of gamma rays depends on the redshift  $z$  and the gamma ray energy  $E_\gamma$  is parametrized by

$$\tau_{bkg\gamma\gamma}(E_\gamma, z) = z^{1.33} (E_\gamma/E_0)^{3/2} \quad (13)$$

where  $E_0 = 90$  GeV. The attenuation rate versus energy is plotted for different redshifts in Fig. 3. The continuous lines show the parametrization given in Eq. 13, whereas the dashed lines represent the best fit model by Kneiske et al. (2004). Stecker et al. (2006)'s recent calculations of intergalactic gamma-ray absorption making use of new Spitzer and GALEX data diverge from those of Kneiske & Mannheim (2005) at the higher redshifts due to the recent discovery that active star formation was taking place in young galaxies at redshifts out to beyond 6. This gives larger optical depths at the higher redshifts than previously thought.

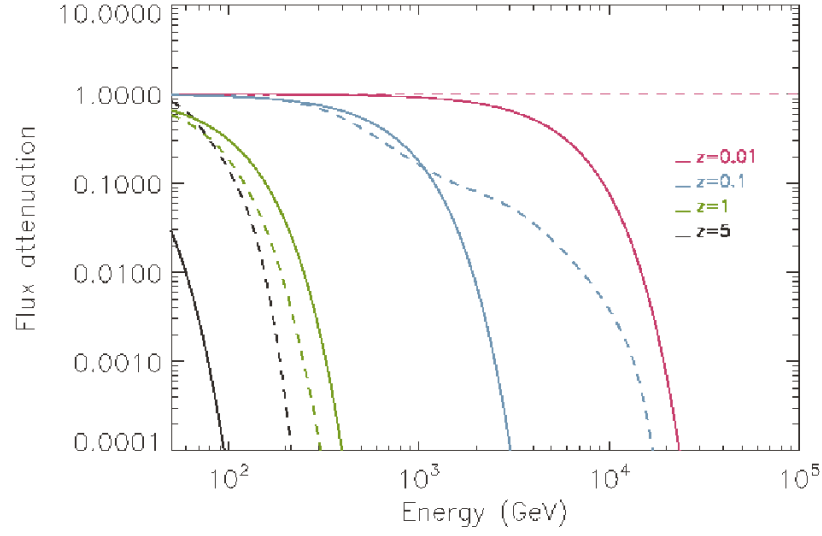


Fig. 3.— Attenuation of  $\gamma$ -ray spectra through  $\gamma\gamma$  absorption at different redshifts. The continuous lines show the parametrization of Eq. 13 and the dashed lines the best fit model of Kneiske et al. (2004).

#### 4. Prompt and scattered emission

Throughout the rest of the paper we will assume that both the synchrotron and the higher energy GRB spectrum have spectral indices  $\alpha = -1$  and  $\beta = -2$ . Also we will consider GRB having time variability of 1 seconds and duration of 20 seconds and a bulk Lorentz factor of 316.

Inside and outside the GRB, the spectrum is assumed to be only attenuated by  $\gamma\gamma$  reactions and the flux which leaves the source and is observed at a luminosity distance  $D_L(z)$  is

$$\frac{dN_{\gamma_{prompt}}}{dE_{\gamma} dt dA}(E_{\gamma}, z, L_{iso}) = \frac{L_{iso}}{4 \pi D_L^2(z) E_{pk}} f(E_{\gamma}) e^{-\tau_{grb \gamma\gamma}(E_{\gamma})} e^{-\tau_{bkg \gamma\gamma}(E_{\gamma}, z)} \quad (14)$$

where

$$f(E_{\gamma}) = \frac{1}{n'_{\gamma} \Gamma_b} \frac{dN'_{\gamma}}{dE'_{\gamma}} \quad (15)$$

and  $\tau_{grb \gamma\gamma}$  and  $\tau_{bkg \gamma\gamma}$  are the optical depths for pair production inside and outside the source.

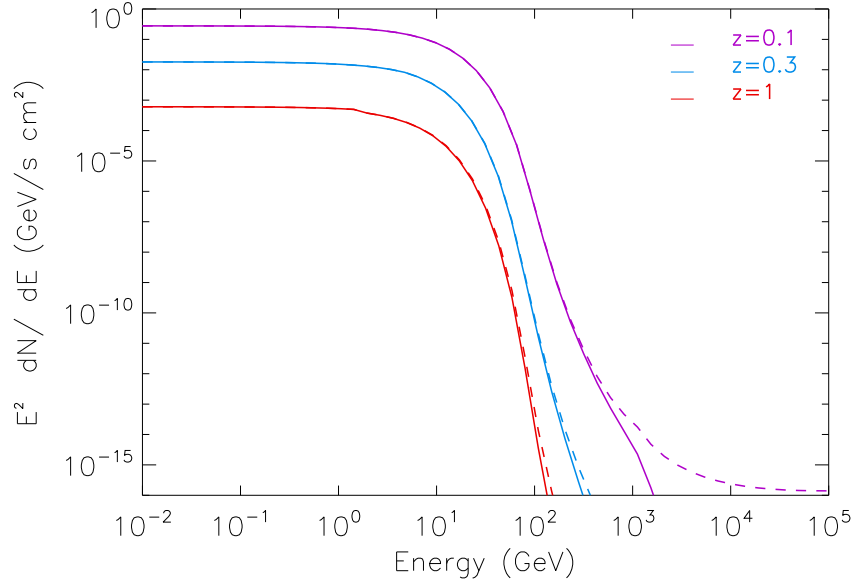


Fig. 4.— Synchrotron and higher energy prompt flux from one GRB having isotropic luminosity  $10^{52}$  erg/s, bulk Lorentz factor 316 and time variability 1 second. The slopes  $\alpha = -1$  and  $\beta = -2$  for both synchrotron and IC spectra. The ratio between the synchrotron peak flux and the TeV emission peak flux is assumed to be 10. The solid lines represented the fluxes attenuated by  $\gamma\gamma$  absorption inside and outside the sources which are located at redshifts 0.1, 0.3 and 1. The dashed lines indicate the fluxes after attenuation inside the GRB.

Outside the GRB, due to  $\gamma\gamma$  interactions with cosmic infra-red background photons (IR) and the cosmic microwave background photons (CMB), most of the high energy photons produce high-energy  $e^\pm$  pairs. We assume that each lepton of the pair shares half of the energy of the initial GRB photon,  $E_e = E_\gamma/2$ . The electron-positron flux from the synchrotron and the IC fluxes from one GRB at a distance  $D_L(z)$  in the observer's frame is

$$\left(\frac{dN_e}{dA dE_e dt}(E_e, z, L_{iso})\right)_{grb} = 2 \frac{L_{iso}}{4\pi D_L^2(z)} \frac{f(E_\gamma)}{E_{pk}} e^{-\tau_{grb\gamma\gamma}(2E_e)} [1 - e^{-\tau_{bkg\gamma\gamma}(2E_e, z)}] \quad (16)$$

The pair flux will be enriched as long as the burst lasts. The time integrated electron-positron fluxes are given by

$$\left(\frac{dN_e}{dA dE_e}\right)_{grb} = \int_0^T dt \left(\frac{dN_e}{dA dE_e dt}\right)_{grb}. \quad (17)$$

The pairs will inverse Compton scatter off CMB and IR photons and produce secondary photons, which will in turn interact with IR photons and generate other pairs. Multiple inverse Compton scatterings will happen until the energy of the secondary photons is no longer sufficient to trigger a pair production with the IR photons. When the energy of the scattered photons is insufficient to produce a subsequent pair, the photons will travel to the detector without undergoing further absorption. When simulating the series of inverse Compton scatterings we assume that all interactions happen very close to the source, at the redshift of the source itself. We also assume that the magnetic field is stronger than  $10^{-16}$  Gauss in order for the flux to be isotropically radiated. The number of secondary photons per unit volume per photon energy interval created in the vicinity of a GRB through one inverse Compton scattering of the pairs in Eq.(16) off cosmic of the background radiation photons is Gaisser (1990)

$$\begin{aligned} (q_{IC}(E_\gamma, z, L_{iso}))_{grb} &= \left(\frac{dN_\gamma}{dE_\gamma dV}\right)_{grb} \\ &= \int dE_e \int d\epsilon_{cmb} \frac{d\sigma_{IC}}{dE_\gamma}(E_\gamma, E_e \epsilon_{cmb}) u_{cmb}(\epsilon_{cmb}, z) \left(\frac{dN_e}{dA dE_e}\right)_{grb} \end{aligned} \quad (18)$$

where  $\frac{d\sigma_{IC}(E_\gamma, E_e, \epsilon_{cmb})}{dE_\gamma}$  can be either the differential Thomson cross section (for low energy pairs) or the differential Klein-Nishina formula (for high energy pairs) (Schlickeiser 2003),  $u_{cmb}(\epsilon_{cmb}, z)$  is the density of CBR photons per unit volume per photon energy interval at redshift  $z$  (Peebles 1976). If inverse Compton scattered photons have a high enough energy, they will be absorbed by the IR photons.

In order to evaluate the contribution from scattered  $\gamma$ -ray emission from all GRBs we

input the observed GRB redshift distribution (Guetta et al. 2005; Firmani et al. 2004)

$$n_{GRB}(z) = \frac{R_{GRB}(z)}{1+z} \frac{dV}{dz} \int d \log(L_{iso}) \Phi_0(L_{iso}). \quad (19)$$

In Eq.(19),  $\Phi_0(L_{iso})$  is the luminosity function, defined as the comoving space density of GRBs in the interval  $\log(L_{iso})$  and  $\log(L_{iso}) + d \log(L_{iso})$ . Following Schmidt (1999), we derive the luminosity function  $\Phi_0(L_{iso})$  by assuming a broken power law with lower and upper limit,  $L_{lower} = \frac{L_{iso}^*}{30}$  and  $L_{upper} = 10 L_{iso}^*$ , respectively, where  $L_{iso}^* = 4.4 \cdot 10^{51}$  erg/s,

$$\Phi_0(L_{iso}) = \begin{cases} a \left(\frac{L_{iso}}{L_{iso}^*}\right)^{\gamma_1} & \text{for } L_{lower} < L_{iso}^* < L_{upper} \\ a \left(\frac{L_{iso}}{L_{iso}^*}\right)^{\gamma_2} & \text{for } L_{lower} < L_{iso}^* < L_{upper} \end{cases} \quad (20)$$

The normalization constant  $a$

$$a = \frac{1}{\frac{1}{\gamma_1} \left(1 - \frac{1}{\delta_1^{\gamma_1}}\right) + \frac{1}{\gamma_2} \left(-1 + \delta_2^{\gamma_2}\right)} \quad (21)$$

is obtained by imposing the integral of  $\Phi_0(L_{iso})$  to give unity. We assume  $\gamma_1 = -0.1$ ,  $\gamma_2 = -2$ ,  $\delta_1 = 30$  and  $\delta_2 = 10$ .

The integration over  $L_{iso}$  is performed over the interval indicated in Guetta et al. (2005). In Eq.(19) the redshift distribution of GRBs  $R_{GRB}(z)$  is

$$R_{GRB}(z) = \frac{23 e^{3.4z} \rho_{GRB} G(z, \Omega_m, \Omega_\Lambda)}{22 + e^{3.4z}} \quad (22)$$

where

$$G(z, \Omega_m, \Omega_\Lambda) = \frac{\sqrt{\Omega_m (1+z)^3 + \Omega_k (1+z)^2 + \Omega_\Lambda}}{(1+z)^{3/2}} \quad (23)$$

and  $\rho_{GRB} = 0.44 \text{ Gpc}^{-3} \text{ yr}^{-1}$  is the observed rate of GRB per differential co-moving volume.

$$\frac{dV}{dz} = \frac{d_h (1+z)^2 d_a^2 d\Omega}{\sqrt{\Omega_m (1+z)^3 + \Omega_k (1+z)^2 + \Omega_\Lambda}}. \quad (24)$$

where  $d_a$  is the angular diameter distance and  $d_h$  is the Hubble distance.

The secondary source function in Eq.(18), iterated over multiple scatterings, is integrated over the comoving line of sight distance  $dl$

$$dl = d_h \frac{dz}{\sqrt{\Omega_m (1+z)^3 + \Omega_k (1+z)^2 + \Omega_\Lambda}} \quad (25)$$

and weighted over the number of GRBs  $n_{GRB}$  per unit time to obtain the total counting rate of the diffuse background flux

$$F_{scattered} = \frac{dN_{\gamma scattered}}{dA dE_{\gamma} dt} = \int dl \int dz (q_{IC}(E_{\gamma}, z, L_{iso}))_{grb} n_{GRB}(z) e^{-\tau_{bkg\gamma\gamma}(E_{\gamma}, z)} \quad (26)$$

where the integration over the redshift is performed from redshift 0.01, corresponding to about 40 Mpc, to redshift 10. As we mentioned earlier if we assume that the intergalactic magnetic field is stronger than  $10^{-16}$  Gauss the beamed emission from GRBs is isotropically radiated. So the flux contribution for each burst is lower by the beaming solid angle divided by  $4\pi$ . However there are more GRBs, increased by  $4\pi$  divided by the beaming solid angle, which contribute to the diffuse background. So the two beaming factor corrections cancel out and the unknown beaming fraction does not influence Eq.(26).

The total flux from the prompt GRB emission is given by the following integral

$$F_{prompt} = \frac{dN_{\gamma prompt}}{dA dE_{\gamma} dt} = \int dz \left( \frac{dN_{\gamma prompt}}{dE_{\gamma} dA} \right)_{grb} n_{GRB}(z) e^{-\tau_{bkg\gamma\gamma}(E_{\gamma}, z)} \quad (27)$$

where

$$\left( \frac{dN_{\gamma prompt}}{dE_{\gamma} dA} \right)_{grb} = \int_0^T dt \left( \frac{dN_{\gamma prompt}}{dE_{\gamma} dt dA} \right)_{grb} \quad (28)$$

is the differential gamma ray prompt flux from each GRB in Eq.(14), measured in  $\text{GeV}^{-1}\text{cm}^{-2}$ ,  $n_{GRB}(z)$  is the redshift dependent number of GRBs per unit time given in Eq.(19).

In Fig. 5 we plot the sum of the prompt and scattered GRB emissions assuming an average value of the bulk Lorentz factor equal to 316. The average time variability of the bursts is assumed to be 1 second and the duration 20 seconds. The input energy flux at the high energy peak  $E_{pk2}$  is assumed 10 times stronger than that at the synchrotron peak  $E_{pk}$ , i.e.  $R = 10$  (see Fig. 1).

For higher average bulk Lorentz factors  $\Gamma_b$ , the pair production inside the GRB source region is less efficient and therefore the  $\gamma$ -ray flux escaping the GRBs will be higher and both the prompt and the scattered fluxes in Fig. 5 will be higher. If the average time variability  $\delta t$ , which is related to the dimensions of the GRB shock radius, is lower, then the number of photons emitted through electron synchrotron emission inside the GRB source region is higher and consequently we expect higher prompt and scattered fluxes. The second peak energy  $E_{pk2}$  is the energy at which we expect the maximum TeV energy flux and, as pointed out, is constrained by the observed synchrotron spectrum to be between  $10^5$  and  $10^6$  times the synchrotron peak energy  $E_{pk}$ . If we consider a lower value of  $E_{pk2}$ , we have more photons at lower energies which scatter off the CBM and IR photons and therefore

the cascade processes started by the GRB photons off the interstellar radiation fields will be interrupted sooner and will produce lower scattered photon fluxes. A lower second peak energy  $E_{pk2}$  might also imply a more efficient pair production absorption inside the GRB source region, as shown in Fig. 2. Finally assuming a shorter average time duration  $T$  for the GRBs less photons will be injected by the GRBs and the scattered flux will be lower.

As a back of the envelope calculation, by assuming that the average amount of energy released by each GRB is of the order of  $10^{51} \text{ erg}$ , the GRB rate is one per day and the average redshift is 1, the total flux emitted by all GRBs is roughly of the order of  $5 \times 10^{-9} \text{ GeV cm}^{-2} \text{ s}^{-1} \text{ sr}^{-1}$ . This is roughly consistent with our more rigorous calculations.

## 5. Conclusions and discussion

Current limits for the contribution of blazars and other sources to the extragalactic diffuse emission indicate that between 25 and 50 per cent of the extragalactic diffuse emission is not explained yet and, in principle, can be due to any other unresolved source outside the Galaxy (Sreekumar et al. 1998; Mukherjee & Chiang 1999; Hartmann et al. 2003; Strong et al. 2004; Kneiske & Mannheim 2005; Stecker & Salamon 1996, 2001; Dar & Shaviv 1995; Loeb & Waxmax 2000; Stawarz et al. 2006). The prompt and scattered emissions from GRBs should contribute to the diffuse extragalactic emission, too. In fact, outside the GRB source, due to interactions with cosmic infra-red background photons, most of the high energy GRB photons produce high-energy electron-positron pairs. The pairs inverse Compton scatter off CMB photons and produce electromagnetic cascades. In this way the beamed GeV-TeV GRB emission is re-processed and converted into an isotropic MeV energy emission, which contributes to the extragalactic diffuse emission.

We have modeled the emission from GRBs as due a low energy synchrotron spectrum and a higher energy IC spectrum. The IC spectrum extends up to Klein-Nishima limit. Also we have assumed the higher energy IC emission from GRBs to be 10 times stronger than the lower energy standard synchrotron emission. This assumption is equivalent to requiring that the GRB inverse Compton Y-parameter is equal to 10. Using the BATSE peak flux distribution Guetta et al. (2005) derived the GRB luminosity function assumed for our estimates. The luminosity function can be approximated by a broken power law with a break peak luminosity of  $4.4 \times 10^{51} \text{ erg ss}^{-1}$ , a typical jet angle of 0.12 rad, and a local GRB rate of  $0.44 h^3 \text{ Gpc}^{-3} \text{ yr}^{-1}$ . Using the redshift and luminosity distributions derived by Guetta et al. (2005) we have summed up the prompt and scattered emissions from all GRBs in the universe. The sum of the prompt and scattered emission from all GRBs is shown in Fig. 5 for a particular choice of GRB parameters. From our optimistic model the  $\gamma$ -ray



emission from prompt and scattered GRB emissions can provide only a small fraction of the extragalactic diffuse emission at EGRET energies and cannot therefore explain the missing flux. From Fig. 5 the sum of prompt and scattered emission from synchrotron and 10 times stronger IC emissions from all GRBs is less than the part of the extragalactic diffuse emission not explained by blazars, admitting that the blazars explain between 25 and 50 percent of the isotropic extragalactic emission. Our optimistic GRB model does not overproduce the extragalactic  $\gamma$ -ray background. We can thus conclude that TeV energy prompt fluxes from GRBs can be at least 10 times bigger than the synchrotron flux without violating the limit imposed by the extragalactic diffuse emission. In allowing TeV energy fluxes from GRBs of comparable or even stronger intensity to the MeV fluxes, our result is consistent with those models (Pe’er & Waxman 2004) which predict fluences at TeV energies similar to those at MeV energies, the observations of high energy emission from GRB 970417a with Milagro (Atkins et al. 2003) and the analysis of GRB 941017 done by Gonzales et al. (2003), which pointed out the existence of a second flux from GRB 941017 that cannot be explained as synchrotron emission. Experiments like Milagro and future missions like GLAST or mini-HAWC should therefore devote part of their efforts to investigate VHE emissions from GRBs.

We note that the recent Swift detection of GRB 060218 (Campana et al. 2006) suggests that there might be a low-luminosity population of GRBs with a much higher event rate (Liang et al. 2006). On the other hand, these bursts have low luminosities and tend to be X-ray flashes (Campana et al. 2006), which would compensate their high event rate. Future analyses are needed to reveal the contribution from this category of GRBs.

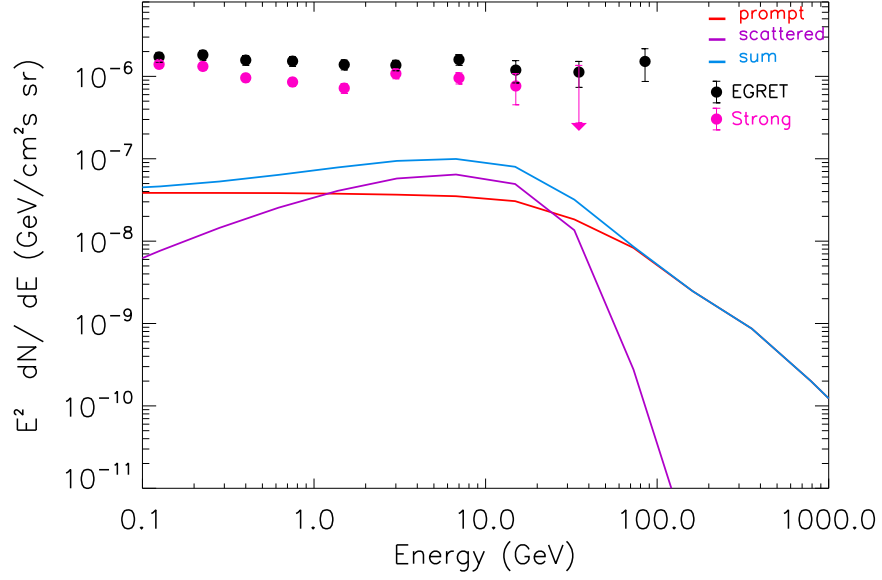


Fig. 5.— GRB Total Emission from bursts having average bulk Lorentz factors 316, time variability 1 second and duration 20 seconds. The slopes  $\alpha = -1$  and  $\beta = -2$  for both synchrotron and IC spectra. The ratio between the synchrotron peak flux and the TeV emission peak flux is assumed to be 10. The flux is attenuated by  $\gamma\gamma$  absorption inside and outside the sources.

The authors would like to thank Pablo Saz Parkinson.

## REFERENCES

- Amati, L. et al., 2002, A&A, 390, 81
- Amenomori, M. et al., 1996, A&A, 311, 919
- Atkins, R. W. et al. 2000, ApJ, 533, L119
- Atkins, R. W. et al. 2003, ApJ, 583, 824
- Band, D. et al. 1993, ApJ, 413, 281
- Baring, M. G. & Harding, A. K. 1997, ApJ, 491, 663
- Beloborodov, A. M. 2005, ApJ, 618, L13
- Böttcher, M. & Dermer, C. D. 1998, ApJ, 499, L131
- Campana, S. et al. 2006, Nature, 442, 1008
- Chi, X. & Wolfendale, A. W., 1989, J. Phys. G: Nucl. Phys. 15,1509
- Coppi, P. S. & Aharonian, F. A., 1997, ApJ, 487, L9
- Dai, Z. G. & Lu, T. 2002, ApJ, 580, 1013
- Dar A., & Shaviv, N., 1995, PRL 75, 3052
- Erlykin, A. D., & Wolfendale, A. W., J. Phys. G. 21, 1149
- Fan, Y.-Z., Dai, Z.-G., Huang, Y.-F. & Lu, T. 2002, ChJAA, 2, 449
- Fan, Y. Z., Zhang, B. & Wei, D. M. 2005, ApJ, 629, 334
- Firmani, C., Avila-Reese, V., Ghisellini, G. & Tutukov, A. V. 2004, ApJ, 611, 1033
- Frail, D. A. et al., 2001, ApJ, 562, L55
- Gaisser, T. 1990, Cosmic rays and particle physics, Cambridge University Press
- Gonzales, M et al., 2003, Nature, 424, 749
- Guetta, D., Piran, T. & Waxman, E. 2005, ApJ, 619, 412

- Hartmann, D. H. et al. 2003, AIPC 662, 477G
- Hogg, D. W. , arXiv:astro-ph/9905116.
- Hurley, K. et al. 1994, Nature, 372, 652
- Kneiske, T. M., Bretz, T., Mannheim, K. & Hartmann, D. H. 2004, A&A, 413, 807
- Kneiske, T. & Mannheim, K. 2005, AIP Conf. Proc. 745, 578
- Kumar, P. & Panaitescu, A. 2003, MNRAS, 346, 905
- Liang, E. W., Zhang, B., Virgili, F. & Dai, Z. G. 2006, ApJ, submitted (astro-ph/0605200)
- Lithwick, Y. & Sari, R. 2001, ApJ, 555, 540
- Loeb, A. & Waxman, E. 2000, Nature 405, 156
- Mukherjee, R. & Chiang J., 1999, APh, 11, 213
- Padilla, L. et al. 1998, A&A, 337, 43
- Panaitescu, A., & Kumar, P. 2001, ApJ, 554, 667
- Peebles, P. J. E. 1976, Principles of Physical Cosmology, Princeton series in Physics
- Pe’er, A. & Waxman, E. 2004, ApJ, 613, 448
- Plaga, R. 1995, Nature, 374, 430
- Protheroe, R. J., & Stanev, T. 1993, MNRAS, 264, 191
- Razzaque, S., Mészáros, P. & Zhang, B. 2004, ApJ, 613, 1072
- Rhoads, J. E. 1999, ApJ, 525, 737
- Rossi, E., Lazzati, D. & Rees, M. J. 2002, MNRAS, 332, 945
- Sari, R., Piran, T. & Halpern, J. 1999, ApJ, 519, L17
- Sari, R., & Esin, A. A. 2001, ApJ, 548, 787
- Schlickeiser, R. 2003, Cosmic ray astrophysics, Springer Verlag
- Schmidt, M. 1999, ApJ, 523, L117
- Sreekumar, P. et al, 1997, AIP Conf. Proc. 410, 344

- Sreekumar, P. et al. 1998, ApJ, 494, 523
- Stawarz, L., Kneiske, T. M., & Kataoka, J., 2006, ApJ, 637, 698
- Stecker F. W. & Salamon, M. H., 1996, ApJ, 464, 600
- Stecker F. W. & Salamon, M. H., 2001, AIP PC 587, 432
- Stecker F. W., Malkan, M. A. & Scully, S. T. ApJ, 648, 774
- Strong, A. W., Moskalenko, I. V. & Reimer, O. 2004, ApJ, 613, 956
- Wang, X. Y. et al, 2001, ApJ, 556, 1010
- Wang, X. Y., Cheng, K. S., Dai, Z. G. & Lu, T. 2004, ApJ, 604, 306
- Wang, X. Y., Li, Z. & Mészáros, P. 2006, ApJ, 641, L89
- Wdowczyk, J. & Wolfendale, A. W., 1990, ApJ, 349, 35
- Zhang, B., Fan, Y. Z., Dyks, J. et al. 2006, ApJ, 642, 354
- Zhang, B., Kobayashi, S. & Mészáros, P. 2003, ApJ, 595, 950
- Zhang, B. & Mészáros, P. 2001, ApJ, 559, 110
- Zhang, B. & Mészáros, P. 2002a, ApJ, 581, 1236
- Zhang, B. & Mészáros, P. 2002b, ApJ, 571, 876